

Article

## Isotopological Supramolecular Networks from Melamine and Fatty Acids

Hermann Walch, Anne-Kathrin Maier, Wolfgang M. Heckl, and Markus Lackinger

*J. Phys. Chem. C*, **2009**, 113 (3), 1014-1019 • DOI: 10.1021/jp8078474 • Publication Date (Web): 29 December 2008

Downloaded from <http://pubs.acs.org> on March 11, 2009

### More About This Article

---

Additional resources and features associated with this article are available within the HTML version:

- Supporting Information
- Access to high resolution figures
- Links to articles and content related to this article
- Copyright permission to reproduce figures and/or text from this article

[View the Full Text HTML](#)

# Isotopological Supramolecular Networks from Melamine and Fatty Acids

Hermann Walch,<sup>\*,†</sup> Anne-Kathrin Maier,<sup>†</sup> Wolfgang M. Heckl,<sup>†,‡</sup> and Markus Lackinger<sup>\*,†</sup>

Department for Earth and Environmental Sciences and Center for NanoScience (CeNS), Ludwig-Maximilians-University Munich, Theresienstr. 41, D-80333 München, Germany, and Deutsches Museum, Museumsinsel 1, D-80538 München, Germany

Received: September 4, 2008; Revised Manuscript Received: October 27, 2008

The formation of bimolecular isotopological monolayers comprised of melamine and members of the homologous series of fatty acids extending from pentanoic through tridecanoic acid was studied at the liquid–graphite interface by scanning tunneling microscopy. In these systems, the fatty acids not only serve as solvents, i.e., provider and transport medium for solute molecules, but are also a structure determining part of the self-assembled monolayers. For all solvents, hexagonal structures were observed where the lattice parameter increases linearly with the chain length of the fatty acid from 2.8 nm for pentanoic acid to 4.1 nm for tridecanoic acid. All bimolecular networks exhibit the same topology: the basic unit consists of a melamine hexamer which is stabilized by internal N···H–N hydrogen bonds and surrounded by 12 radially arranged fatty acid molecules. The *p6* symmetry of the monolayer originates from the melamine core, whereas the lattice parameter is determined by the aliphatic chain length of the fatty acid. For a deeper insight into the relative energetics, all experimentally observed structures were simulated by force-field calculations

## Introduction

Isotopological structures share the same building plan, but the size, i.e., in case of crystalline systems the lattice parameter, is variable due to different dimensions of interchangeable constituents. Scalability, as a general, widely encountered concept and principle, has always attracted much attention. Particularly in material science scalability is a very intriguing property since it may allow for the gradual variation of specific material properties. Also, in many cases, the synthesis follows the same pathway for all structures. Prominent examples are the iso reticular–metal organic frameworks (IR-MOFs), discovered and characterized by Yaghi et al.<sup>1</sup> There, a [Zn<sub>4</sub>O]<sup>6+</sup> tetraeder serves as a connection point and various deprotonated para-dicarboxylic acids are the interconnecting spokes. Owing to the  $\bar{4}3m$  symmetry of the connection points, referred to as secondary building units (SBU), most structures are cubic and the lattice constant ranges from 1.29 to 3.43 nm. The accompanying variation in pore diameter makes these mesoporous structures highly interesting for applications in the field of size selection and gas separation.<sup>2</sup> In case of IR-MOFs, the SBUs and organic spokes are interconnected through metal coordination bonds. Likewise, two-dimensional isotopological metal coordination networks were observed for cobalt atoms with dicyanitrile-polyphenyl molecules on Ag(111).<sup>3</sup> Here we present a bimolecular system where the dominating interactions are hydrogen bonds. Despite the relative weakness of hydrogen bonds (here ~6–10 kcal/mol for a 2-fold hydrogen bond) as compared to coordination bonds (typically 10–20 kcal/mol), a remarkable scalability of the system was found and the use of aliphatic spacers facilitates fine-tuning of the lattice parameter.

## Experimental Section

All experiments were conducted with a home-built STM operated by a commercial RHK SPM-100 control system. Tips were mechanically cut from a Pt/Ir wire (90/10). Chemicals were used as received from Sigma-Aldrich without further purification. Saturated solutions were prepared by adding melamine to fatty acids (~5 mL) until precipitation occurs. A small droplet (~10  $\mu$ L) of solution was then applied to the freshly cleaved basal plane of highly oriented pyrolytic graphite (HOPG) substrates. Topographs were obtained in the constant current mode of operation with the tip immersed into solution. Since fatty acids from decanoic acid on are already solid at room temperature, a heatable sample holder was used which enables imaging at sample temperatures up to ~60 °C. The heating stage consists of a resistance wire embedded into thermally conducting epoxy resin and is thermally well isolated from the instrument. Careful shielding and a high electrical resistance of the heating wire (diameter 0.045 mm), i.e. low driving currents (typically ~30 mA), minimize cross-talk with the signal. The graphite sample is directly attached to the heating stage and a dc heating power of ~0.3 W is sufficient to maintain surface temperatures around ~50 °C. For decanoic through tridecanoic acid, solutions were saturated at ~50 °C and directly applied to the preheated sample holder. Before the coarse approach, the tip is immersed into solution and allowed to thermally equilibrate for ~10 min. This procedure is necessary to reduce lateral and vertical thermal drift. In order to exclude artifacts due to thermal drift and nonideal piezo behavior, adsorbate lattice parameters were precisely determined by means of calibration images, where both the monolayer and the underlying graphite were imaged within one frame.

## Results and Discussion

Melamine is a heterocyclic aromatic molecule and consists of a triazine ring endowed with three amine groups at the 2, 4, and 6 positions. Melamine is well functionalized for intermo-

\* To whom correspondence should be addressed. E-mail: hermann.walch@physik.unimuenchen.de; markus@lackinger.org.

<sup>†</sup> Ludwig-Maximilians-University Munich.

<sup>‡</sup> Deutsches Museum.

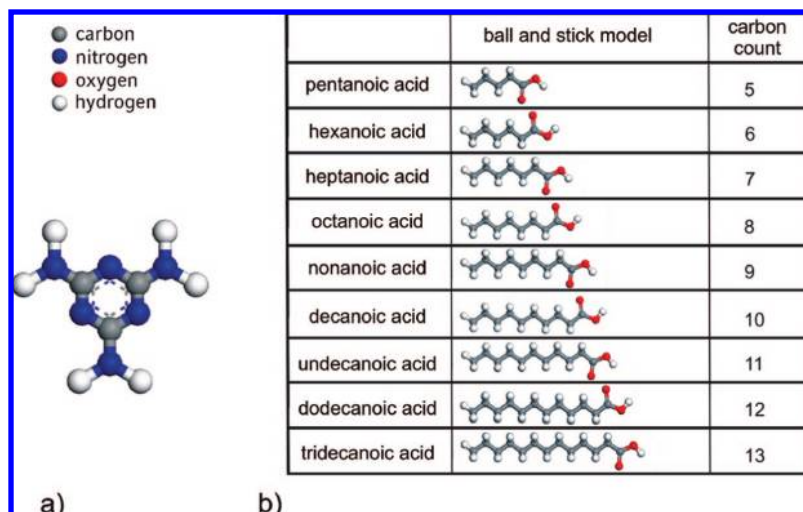


**Figure 1.** Chemical structures of (a) melamine and (b) the homologous series of 1-fatty acids used in this study.

lecular hydrogen bonds: amine groups can act as proton donors whereas the nitrogen atoms in the triazine ring can be proton acceptors through their lone pair electrons. In addition, its planar geometry and the aromatic system can give rise to planar adsorption on various substrates, a prerequisite for studying the formation of two-dimensional hydrogen bonded networks.

On surfaces, melamine shows a high affinity to cocrystallize with other organic compounds. Several stable bimolecular structures were found upon coadsorption with PTCDI (perylene-tetracarboxylic-diimide) depending on mixing ratios and post deposition annealing procedures. After the observation of a hexagonal honeycomb network by Theobald et al.,<sup>4</sup> Silly et al. discovered parallelogram structures,<sup>5</sup> and a similarly hexagonal “pinwheel” structure.<sup>6</sup> Experiments with PTCDA (3,4,9,10-perylene-tetracarboxylic-dianhydride) instead of PTCDI yielded row-like structures.<sup>7</sup> Also cyanuric acid has been found to be a very suitable coadsorbant for melamine.<sup>8,9</sup> Both cyanuric acid and melamine were observed to self-assemble into stable monolayers by themselves.<sup>10,11</sup> For melamine, chiral and non-chiral monolayer structures were found, all based on 2-fold hydrogen bonds between adjacent molecules. The chiral structure is comprised of cyclically hydrogen bonded melamine hexamers where perpendicularly adsorbed melamine guest molecules were observed at the center.<sup>12</sup> Yet, all studies above were carried out under ultrahigh vacuum conditions with samples prepared by vapor deposition whereas the results presented here have been obtained at the liquid–solid interface. In contrast, molecules adsorbed at the liquid–solid interface can be in equilibrium with dissolved molecules and growth is often thermodynamically controlled, which renders the preparation of bimolecular networks more challenging.<sup>13</sup> Similar to melamine, fatty acids can also act as acceptors and donors for hydrogen bonds through their carboxylic functionality.<sup>14</sup> Moreover, their total length can be varied in increments of  $\sim 0.13$  nm by adding further  $\text{CH}_2$  groups to the alkane tail. In this work, all members of the homologous series between pentanoic and tridecanoic acid were found to cocrystallize with melamine at the solution–graphite interface.

An example of a well ordered hexagonal structure obtained with melamine in octanoic acid is depicted in Figure 2. The lattice parameter accounts to 3.3 nm and the contrast exhibits a hexagonal arrangement of 1.8 nm wide dark circular depressions separated by elevated (bright) walls. Similar topographs of

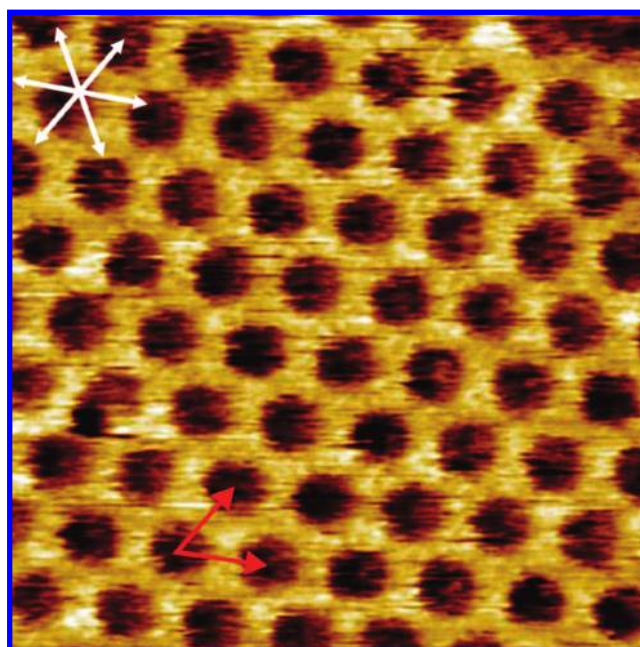


**Figure 2.** STM topograph obtained from melamine dissolved in octanoic acid at room temperature ( $25 \times 25 \text{ nm}^2$ ) with  $U_T = 1.0 \text{ V}$ ,  $I_T = 70 \text{ pA}$ . The structure is hexagonal with a lattice parameter of 3.3 nm, adsorbate lattice vectors are marked by red arrows. The white arrows in the upper left corner indicate the main axes of the underlying graphite substrate as deduced from calibration images.

hexagonal structures were obtained for all nine fatty acids investigated (cf. Supporting Information for a full set of topographs). For pentanoic through nonanoic acid, experiments were performed at room temperature, whereas for decanoic acid through tridecanoic acid, a sample temperature above the melting point of the respective solution was maintained by means of the heatable sample holder. Interestingly, as illustrated in Figure 3, a linear relation between the number of carbon atoms in the fatty acid solvent (referred to as carbon count) and the lattice parameter of the interfacial hexagonal monolayer was found.

A linear fit resulted in a slope of 0.15 nm/(carbon count) which corresponds to the increment of the lattice parameter from one fatty acid to the next higher one. Since the lattice parameter is a function of applied solvent and both contrast and symmetry

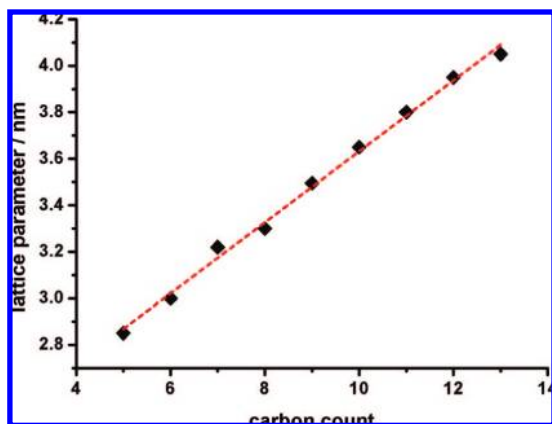


**Figure 3.** Dependency of experimentally determined lattice parameters of the hexagonal networks on the number of carbon atoms in the fatty acid solvent (carbon count). Lattice parameters were deduced from calibrated STM images and averaged over independent experimental runs. They range from  $(2.8 \pm 0.1)$  nm for pentanoic acid to  $(4.1 \pm 0.1)$  nm for tridecanoic acid. The slope of the linear fit ( $R^2 = 0.995$ ), i.e., the increase of lattice parameter per additional carbon atom in the alkane tail of the solvent, corresponds to  $(0.15 \pm 0.01)$  nm/(carbon count).

of the monolayer are entirely different from the row like structure of pure fatty acid monolayers,<sup>15–17</sup> the formation of bimolecular networks comprised of melamine and solvent molecules can be concluded. Because the overall length of the fatty acid molecules also increases linearly with carbon count, it is very likely that the solvent accounts for the scalability of the network. Consequently, the symmetry of the monolayer is related to the trigonal symmetry of melamine possibly in combination with the hexagonal symmetry of the substrate. Surprisingly, with phenyloctane used as solvent no pure melamine monolayers could be observed, despite the molecule's capability to form extended hydrogen bonded sheets as observed on Au(111).<sup>11</sup> Also with iso-alcohols (nonanol, decanol, and undecanol) as solvents, only pure solvent monolayers were observed but no coadsorption with melamine. Apparently, the stabilizing influence of an additional compound with a relatively strong bond to melamine is required for melamine monolayer formation at the liquid–graphite interface. For two reasons fatty acids are very appropriate: first, they can form two hydrogen bonds ( $O\cdots H-N$  and  $O-H\cdots N$ ) per molecule with melamine and not only one as alcohols; second, the almost perfect registry between the alkane backbone and the graphite substrate leads to high adsorption energies for fatty acids which increase linearly with chain length. Remarkably, fatty acids which usually serve as a standard solvent for self-assembly of carboxylic acids at the liquid–solid interface have now become a structure determining part of a bimolecular self-assembled system.<sup>18,19</sup>

Proposing a structural model for the monolayer based on the STM contrast is a crucial task, especially when the unit cell is rather large and contains more, possibly different molecules. Normally, the contrast is interpreted based on the geometry, size, and electronic structure of the adsorbed molecules, but high resolution images are required. In this study, we reproducibly observe different STM contrasts rather dependent on the specific tip than systematically on applied tunneling bias. Representative images obtained in nonanoic acid are depicted in Figure 3a–c; similar observations were made with the whole homologous series of fatty acids. For a given system, the lattice parameters are similar for all contrast types.

In analogy to the structure of previously observed bimolecular networks, an open pore structure with a periodic arrangement

of supramolecular cavities might be concluded from contrast I. However, it is significant that the walls which separate the putative cavities appear relatively thick compared to other open-pore networks. Contrast II is inverted with respect to I. Instead of apparent depressions, hexagonally arranged, 1.8 nm wide bright patches with a distinct 6-fold internal symmetry are observed. It is noteworthy that the size of both the dark features in contrast I and the bright features in II does not vary for the homologous row of solvents. Contrast III also consists of hexagonally arranged apparent depressions. However, as opposed to contrast I, the separating walls are better resolved and reveal internal features. As indicated in Figure 3c, each apparent depression is bordered by six bright bars. Again, these larger bars are comprised of four clearly discernible bright parallel elongated features, about 1 nm long for the nonanoic acid system. The internal parts are not as well resolved as in the case of contrast II, but still exhibit fine structure.

As the size of the putative cavities remains constant for all systems it is reasonable to assume that this part of the structure consists of the invariable compound, namely melamine. Size and symmetry is consistent with a melamine hexamer (1.8 nm in diameter) which is stabilized by 12 cyclical internal  $N\cdots H-N$  hydrogen bonds and commonly found as a structure defining unit both in pure melamine monolayers<sup>11</sup> and bimolecular networks.<sup>6</sup>

Since the increment of the lattice parameter within the experimental error is similar to the length increment of the fatty acids it is reasonable to assume that the alkane tail is nearly aligned with the adsorbate lattice vector. Also, the size of the bright elongated features in contrast III corresponds to the size of the respective fatty acid for different structures.

A molecular model considering all requirements stated above is presented in Figure 5a. The basic unit is star shaped and consists of six internally hydrogen bonded melamine molecules which form a hexagonal core. Six pairs of fatty acid molecules are radially attached to this core via hydrogen bonds, while the  $p6$  symmetry of the melamine core is preserved. The main contribution for the interaction between adjacent basic units arises from van der Waals interaction of aligned fatty acid molecules. The excellent agreement between the proposed model and the observed image contrast III is verified by the superposition depicted in Figure 5b. The respective orientation to the substrate is determined by alignment of all alkane backbones with the underlying graphite which further stabilizes the structure.<sup>20</sup>

Recently, a very similar “pinwheel” structure was reported for coadsorption of melamine with PTCDI in a 4:3 ratio on Au(111).<sup>6</sup> Likewise, a hydrogen bonded melamine hexamer is surrounded by six PTCDI molecules attached via hydrogen bonds. However, in the melamine + PTCDI “pinwheel” structure, PTCDI molecules are arranged nearly tangential to the melamine hexamer, whereas here the fatty acids point away radially from the center.

Also, the proposed model is consistent with the observed scaling behavior of the lattice parameter and explains the occurrence of the different contrasts: depending on the tip either the aromatic system of the melamine core (contrast II) or the aliphatic alkane tails of the fatty acids (contrast III) are observed. While normally in combined aliphatic and aromatic monolayers the aromatic moieties appear higher in constant current STM topographs,<sup>21</sup> here, depending on the tip condition either melamine or fatty acid molecules are observed, but never both at the same time. Contrast I is also dominated by the fatty acid molecules, but due to poorer tip quality they cannot be resolved

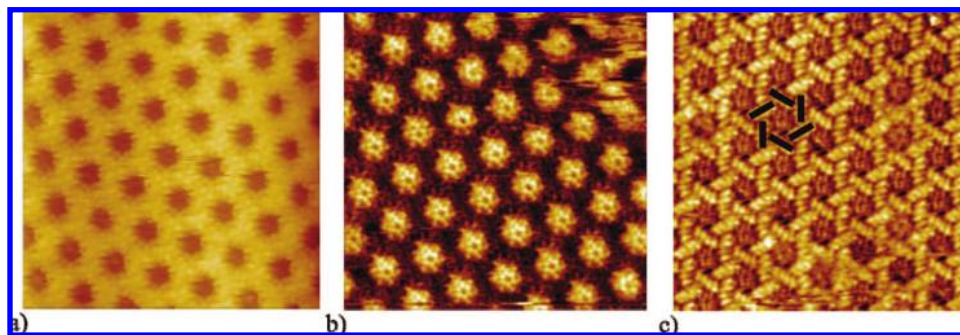


**Figure 4.** Three types of repeatedly observed contrasts, exemplified with the system melamine in nonanoic acid (all images  $20 \times 20 \text{ nm}^2$ ): (a) type I was observed in most experimental runs ( $U_T = 0.7 \text{ V}$ ,  $I_T = 80 \text{ pA}$ ). (b) This particular tip or tip condition causes an apparent inversion, referred to as contrast II: instead of dark depressions a hexagonal arrangement of bright features with internal hexagonal symmetry is resolved ( $U_T = 1.1 \text{ V}$ ,  $I_T = 100 \text{ pA}$ ). (c) Contrast III provides higher resolution of the walls and reveals bright bars arranged in a “pinwheel” structure. Six of those bright bars boarder one dark depression as marked in the image ( $U_T = 1.0 \text{ V}$ ,  $I_T = 110 \text{ pA}$ ).

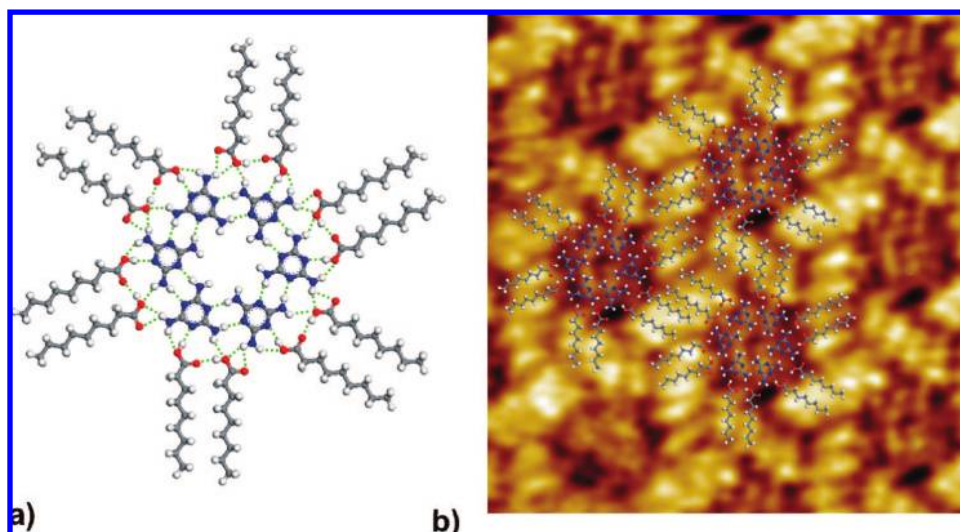


**Figure 5.** (a) Proposed molecular model of the bimolecular network of melamine and nonanoic acid. The symmetry defining connection point is composed of an internally hydrogen bonded melamine hexamer. Twelve fatty acid molecules are radially attached likewise via hydrogen bonds in six parallel pairs and account for the scalability of the system. Hydrogen bonds are indicated by dashed lines (b) full-scale overlay of the proposed model with the STM topograph (image size  $13.8 \times 13.8 \text{ nm}^2$ ,  $U_T = 1.0 \text{ V}$ ,  $I_T = 110 \text{ pA}$ ).

individually as in case of contrast III. No systematic dependency of the contrast on tunneling parameters could be established. Bias dependent imaging with voltages from 0.1 to 1.2 V does not yield different contrasts, while at higher voltages the tunneling current becomes unstable. Yet, erratic switching between contrast I and II frequently occurs, thereby indicating that tip termination is more decisive for the contrast than tunneling voltage.

Although force-field calculations neglect and oversimplify important interactions, they are still a valuable method to compare and discuss the relative energetics, particularly for these isotopological networks where similar molecules and interactions are involved. For the calculation experimentally determined unit cells serve as a constraint and due to the explicit treatment of hydrogen bonds, the Dreiding force-field was used.<sup>22</sup> In order to apply periodic boundary conditions, all unit cells were assumed to be commensurate and convergence could be achieved for all systems. The graphite substrate was approximated by two layers with the atomic positions in the lower layer fixed. An example for an energy optimized melamine + nonanoic acid structure is depicted in Figure 6 (cf. Supporting Information for all other systems). The melamine–melamine and melamine–fatty acid interactions are dominated by hydrogen bonds and obviously remain constant in all systems. In contrast, the fatty acid–fatty acid and fatty acid–graphite interac-

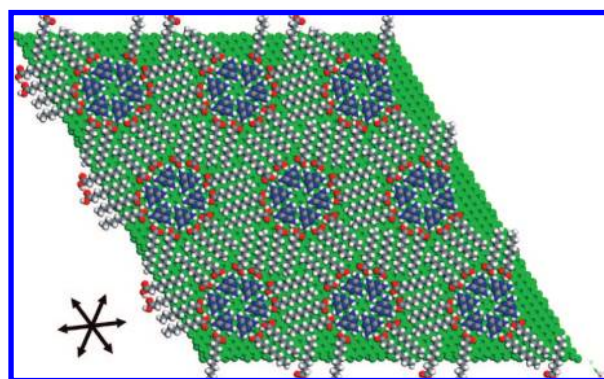


**Figure 6.** Force-field simulation of the system melamine and nonanoic acid, the cut-out depicts  $3 \times 3$  unit cells. Experimentally determined unit cell parameters serve as a constraint and are approximated by a commensurate superstructure matrix in order to facilitate periodic boundary conditions. The main axes of the graphite substrate are indicated in the lower left corner.

tions which are mainly van der Waals type are chain length dependent. Consequently, as can be seen in Figure 7a, the total binding energy per unit cell ( $E_{UC}$ ) increases linearly with carbon count. This behavior can be understood by decomposing the total binding energy into its various contributions: the number of melamine molecules per unit cell, thus their contribution to

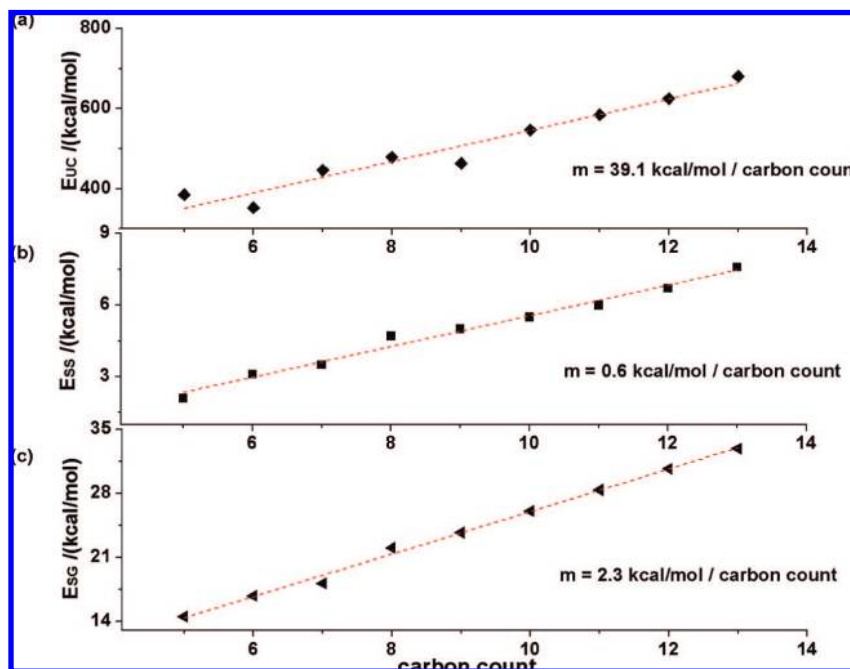


**Figure 7.** Absolute binding energies derived by force-field calculations as a function of fatty acid chain length (carbon count). Dashed red lines represent linear fits and respective slopes are denoted. (a) Total binding energy per unit cell  $E_{UC}$ , i.e., the sum of all molecule–substrate and molecule–molecule interactions, of the melamine + fatty acid system per unit cell. Only the contributions analyzed in more detail in (b) and (c) are dependent on carbon count and account for the linear increase. Melamine related contributions remain constant for all systems. (b) Interaction energy of two geometry optimized solvent molecules  $E_{SS}$  in head-to-tail arrangement. The pure van der Waals interaction also exhibits a linear increase with a slope of 0.6 kcal/mol/carbon count. (c) Adsorption energy  $E_{SG}$  of a single, geometry optimized fatty acid molecule on graphite. The increase per carbon count was determined to be 2.3 kcal/mol

the adhesion energy and the number of hydrogen bonds does not depend on the specific solvent applied. However, both the intermolecular binding energy and the adsorption energy of the fatty acid molecules increase linearly with chain length. Therefore, the linear increase in total binding energy is caused by the fatty acid molecules. In order to verify this hypothesis, the interaction energy of two parallel aligned fatty acid molecules ( $E_{SS}$ ) and the adsorption energies of a single fatty acid molecule ( $E_{SG}$ ) were calculated as a function of carbon count as well, results are depicted in Figure 7, panels b and c. From the calculation it becomes clear that the adsorption energies of the fatty acid molecules are significantly larger than the intermolecular van der Waals binding energies. However, as illustrated in Figure 5a, the fatty acids are also stabilized through a network of hydrogen bonds with the melamine hexamers. The respective binding energy of a pair of fatty acids to the melamine core accounts to 10 kcal/mol. This value is still higher than the 7.8 kcal/mol stabilization energy reported for a melamine dimer by Xu et al.<sup>9</sup> This strong binding between the radial pairs of fatty acids and the melamine hexamer is likely to drive and cause self-assembly of a binary system.

In summary, the total binding energy can be divided into solvent dependent and independent contributions: Independent contributions are melamine–melamine, melamine–substrate, and melamine–fatty acid interactions and remain virtually constant for all solvents. Dependent contributions are fatty acid–fatty acid and fatty acid–substrate interactions and increase linearly with carbon count. Because the lattice parameters and the binding energies per unit cell increase linearly, the binding energies per unit area decrease with one over carbon count, which should render these bimolecular networks thermodynamically unstable for increasing carbon count relative to competing structures such as pure fatty acid monolayers.

In this study the formation of similar bimolecular monolayers of melamine with members of the homologous series of fatty

acids from pentanoic through tridecanoic acid was observed at the liquid–graphite interface. All systems yielded hexagonal structures where the lattice parameter increases linearly with the number of carbon atoms in the fatty acid. The structures are isotopological in the sense that they follow the same building plan: invariant connection points comprised of melamine hexamers account for the hexagonal symmetry. Interconnects of variable length are realized by groups of four fatty acid molecules, where two molecules are hydrogen bonded to the respective connection point and the pairs are held together by van der Waals interaction.

It would be highly interesting to investigate whether the scaling behavior holds for even longer fatty acid molecules. However, their melting point also increases with chain length and stable tunneling conditions could not be achieved for higher fatty acids. Since the melamine hexamers represent a hexagonal arrangement of equally sized aromatic patches in an aliphatic matrix where the next nearest neighbor distance can be fine-tuned in steps of 0.15 nm, it might stimulate further experiments: through selective adsorption of appropriately functionalized nanoparticles, these isotopological networks may act as a structured template which allows for instance to investigate particle–particle interaction as a function of distance with high resolution.

**Acknowledgment.** We gratefully acknowledge financial support by the Deutsche Forschungsgemeinschaft (SFB 486), the Bayerische Forschungsförderung, and the Nanosystems Initiative Munich (NIM).

**Supporting Information Available:** Experimental details, STM topographs, unit cell parameters, and force-field calculations of all nine isotopological networks. This material is available free of charge via the Internet at <http://pubs.acs.org>.

## References and Notes

- (1) Eddaoudi, M.; Kim, J.; Rosi, N.; Vodak, D.; Wachter, J.; O'Keeffe, M.; Yaghi, O. M. *Science* **2002**, *295* (5554), 469–472.
- (2) Yaghi, O. M.; O'Keeffe, M.; Ockwig, N. W.; Chae, H. K.; Eddaoudi, M.; Kim, J. *Nature* **2003**, *423* (6941), 705–714.
- (3) Schickum, U.; Decker, R.; Klappenberger, F.; Zoppellaro, G.; Klyatskaya, S.; Ruben, M.; Silanes, I.; Arnau, A.; Kern, K.; Brune, H.; Barth, J. V. *Nano Lett.* **2007**, *7* (12), 3813–3817.
- (4) Theobald, J. A.; Oxtoby, N. S.; Phillips, M. A.; Champness, N. R.; Beton, P. H. *Nature* **2003**, *424* (6952), 1029–1031.
- (5) Silly, F.; Shaw, A. Q.; Porfyrakis, K.; Briggs, G. A. D.; Castell, M. R. *Appl. Phys. Lett.* **2007**, *91* (25).
- (6) Silly, F.; Shaw, A. Q.; Castell, M. R.; Briggs, G. A. D. *Chem. Commun.* **2008**, (16), 1907–1909.
- (7) Silly, F.; Weber, U. K.; Shaw, A. Q.; Burlakov, V. M.; Castell, M. R.; Briggs, G. A. D.; Pettifor, D. G. *Phys. Rev. B* **2008**, *77* (20).
- (8) Perdigao, L.; Champness, N.; Beton, P. *Chem. Commun.* **2006**, (5), 538–540.
- (9) Xu, W.; Dong, M. D.; Gersen, H.; Rauls, E.; Vazquez-Campos, S.; Crego-Calama, M.; Reinhoudt, D. N.; Stensgaard, I.; Laegsgaard, E.; Linderoth, T. R.; Besenbacher, F. *Small* **2007**, *3* (5), 854–858.
- (10) Kannappan, K.; Werblowsky, T. L.; Rim, K. T.; Berne, B. J.; Flynn, G. W. *J. Phys. Chem. B* **2007**, *111* (24), 6634–6642.
- (11) Silly, F.; Shaw, A. Q.; Castell, M. R.; Briggs, G. A. D.; Mura, M.; Martsinovich, N.; Kantorovich, L. *J. Phys. Chem. C* **2008**, *112* (30), 11476–11480.
- (12) Zhang, H. M.; Xie, Z. X.; Long, L. S.; Zhong, H. P.; Zhao, W.; Mao, B. W.; Xu, X.; Zheng, L. S. *J. Phys. Chem. C* **2008**, *112* (11), 4209–4218.
- (13) Kampschulte, L.; Werblowsky, T. L.; Ravuri, S. K. K.; Schmittl, M.; Heckl, W. A.; Lackinger, M. *J. Am. Chem. Soc.* **2008**, *130* (26), 8502–8507.
- (14) Etter, M. C.; Adsmund, D. A. *Chem. Commun.* **1990**, (8), 589–591.
- (15) Cai, Y. G.; Bernasek, S. L. *J. Am. Chem. Soc.* **2004**, *126* (43), 14234–14238.
- (16) Zhang, H. M.; Yan, J. W.; Xie, Z. X.; Mao, B. W.; Xu, X. *Chem.—Eur. J.* **2006**, *12* (15), 4006–4013.
- (17) Yang, T.; Berber, S.; Liu, J. F.; Miller, G. P.; Tomanek, D. *J. Chem. Phys.* **2008**, *128* (12).
- (18) Tahara, K.; Furukawa, S.; Uji-I, H.; Uchino, T.; Ichikawa, T.; Zhang, J.; Mamdough, W.; Sonoda, M.; De Schryver, F. C.; De Feyter, S.; Tobe, Y. *J. Am. Chem. Soc.* **2006**, *128* (51), 16613–16625.
- (19) Mamdough, W.; Uji-i, H.; Ladislav, J. S.; Dulcey, A. E.; Percec, V.; De Schryver, F. C.; De Feyter, S. *J. Am. Chem. Soc.* **2006**, *128* (1), 317–325.
- (20) Yin, S. X.; Wang, C.; Xu, Q. M.; Lei, S. B.; Wan, L. J.; Bai, C. L. *Chem. Phys. Lett.* **2001**, *348* (3–4), 321–328.
- (21) Lei, S. B.; Yin, S. X.; Wang, C.; Wan, L. J.; Bai, C. L. *Chem. Mater.* **2002**, *14* (7), 2837–+
- (22) Mayo, S. L.; Olafson, B. D.; Goddard, W. A. *J. Phys. Chem.* **1990**, *94* (26), 8897–8909.

JP8078474